A TOPSAR Processor based on the Omega-K Algorithm: Evaluation with Sentinel-1 Data.

Murielle Kirkove, Centre Spatial de Liège, University of Liège, M.Kirkove@ulg.ac.be, Belgium
Anne Orban, Centre Spatial de Liège, University of Liège, aorban@ulg.ac.be, Belgium
Dominique Derauw, Centre Spatial de Liège, University of Liège, dderauw@ulg.ac.be, Belgium
Christian Barbier, Centre Spatial de Liège, University of Liège, cbarbier@ulg.ac.be, Belgium

Abstract

This paper presents a processor for the TOPS (Terrain Observation by Progressive Scans) imaging mode. TOPS signals have two characteristics that make the use of Stripmap SAR processors inconvenient, i.e., azimuth frequency and azimuth time foldings. This paper describes a processor based on the Omega-K (Ω-k) algorithm, combined with pre-processing by frequency unfolding and post-processing by time unfolding. Raw data acquired by Sentinel-1 have been used to assess the quality of image reconstruction.

1 Introduction

Wide swath coverage is essential for many satellite imaging applications. The ScanSAR acquisition mode [1]–[3] satisfies this requirement by periodically steering the antenna beam in the elevation plane in order to image adjacent subswaths, wider coverage being achieved at the price of a loss in azimuth resolution. Besides this trade-off, ScanSAR presents some inconveniences: (1) a modulation of the azimuth signal by the azimuth antenna pattern (AAP), known as scalloping, and (2) a variation of the azimuth ambiguity ratio and signal-to-noise ratio (SNR) with azimuth [2]–[4]. Accordingly, a new wide-swath imaging mode, TOPS (Terrain Observation by Progressive Scans) has been proposed [5]: it consists in steering the antenna beam in the azimuth direction with a constant angular rate from backward to forward, as shown in Figure 1.

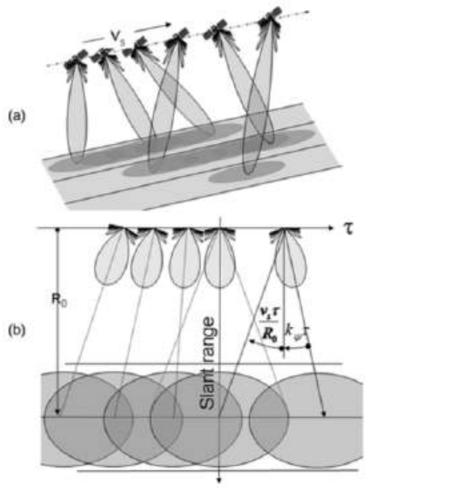

Figure 1: TOPSAR geometry [5]. (a) Three-subswath scanning scheme. (b) Scanning in one sub-swath.

TOPS has been selected as the baseline mode for European Space Agency (ESA)'s Sentinel-1 SAR system [6]. Similar to the ScanSAR acquisition, in TOPS, each sub-swath is divided in the along-track direction into bursts. The duration of these bursts (burst time, T_B) is longer than the footprint time.

TOPS signals have two characteristics that make the use of Stripmap SAR processors inconvenient, i.e., azimuth frequency folding (AzFrF) and azimuth time folding (AzTF). Two generic methods have been proposed in the literature to address these problems, differing on the way the azimuth frequency folding problem is solved, i.e., azimuth sub-aperture (see [7]–[10]) vs. azimuth full aperture (see [5], [11]–[14]).

We present a processor that makes use of the pre- and post-processing full-aperture methods proposed in [5] and [14] respectively, in combination with the Omega-K algorithm [15] as the focusing kernel. The methodology is presented in Section 2. Section 3 shows results based on Sentinel-1 raw data. Section 4 displays our conclusions.

2 TOPS Processing Methodology

2.1 The Azimuth Frequency and Time Folding Problems

Applying classical Stripmap SAR processors to TOPS data results in azimuth-aliased images. This is due to two characteristics of the TOPS signals that are caused by the slope of the Doppler centroid (DC) frequencies along the azimuth direction. The first one is AzFrF: although the beam bandwidth (B_{tD}) is smaller than the azimuth sampling frequency (ν_t), the effective azimuth bandwidth spanned during a burst ($B_{tB,e}$) is larger than B_{tD}, so that the sampling criterion for ν_t (i.e., $B_{tB,e} > \nu_t$) is

ISBN 978-3-8007-4228-8 / ISSN 2197-4403

not fulfilled. The number of times AzFrF occurs is $N_{ff}=B_{tB,e}/v_t$. The second characteristic is AzTF: each burst has a time duration T_B much shorter than the output image (T_{of}), so that one target (with dwell-time indicated by T_D) can be imaged at two azimuth times. The number of times AzTF occurs is $N_{ft}=T_{of}/T_B$.

The sub-aperture method solves the AzFrF problem by dividing the azimuth data into blocks (sub-apertures). Then, the data are focused and post-processed for each aperture, combined, and, possibly post-processed again. The sub-aperture processing methods [7]–[9] use the Chirp-Scaling algorithm as the focusing kernel.

In most of full-aperture methods, azimuth processing consists in three successive steps: (1) pre-processing to deal with the AzFrF problem, (2) focusing with a conventional SAR algorithm, and (3) post-processing to deal with the AzTF problem. As far as we know, only the full-aperture method proposed in [16] is not based on this scheme. It is a generalization of the traditional polar formation algorithm, working for the sliding spotlight and TOPS imaging modes.

Three generic and some specific approaches of pre-processing have been proposed. They are collected in Table 1. The generic ones are: (1) frequency and time scalings (FrTSc), (2) de-ramping (DeRamp), and (3) frequency un-folding (FrUnf). Two variants of Chirp-scaling exist for complete and partial azimuth focusing, respectively. Partial focusing with Chirp-scaling preserves the initial time-frequency distribution (TFDi), complete focusing with Chirp-Scaling or Omega-K does not. Only the methods using FrTSc or FrUnf as pre-processing and complete focusing have a generic post-processing form, called time un-folding (TUnf), the other ones are specific. Table 1 lists the TOPS full-aperture processing methods that are state-of-the art and their components grouped in categories.

Categories		Methods (see references)			
		[14]	[13]	[5]	[17]
Pre-processing	FrTSc	■			
	DeRamp		■		
	FrUnf			■	
	Specific				■
SAR focusing	Chirp-Scaling	■	■		■
	Omega-K			■	
Post-processing	TUnf	■		■	
	Specific		■		■

Table 1: List of full-aperture TOPS processings and their components grouped in categories.

2.2 Proposed processing

The proposed TOPS processor is a full-aperture method that combines (1) a pre-processing step based on the full-aperture method of ref. [5], that we shall refer to as frequency unfolding (FrUnf); (2) the Omega-K processing; and (3) post-processing based on the full-aperture method described in ref. [14], that we shall refer to as time unfolding (TUnf). The block diagram of the processor is shown in Figure 2.

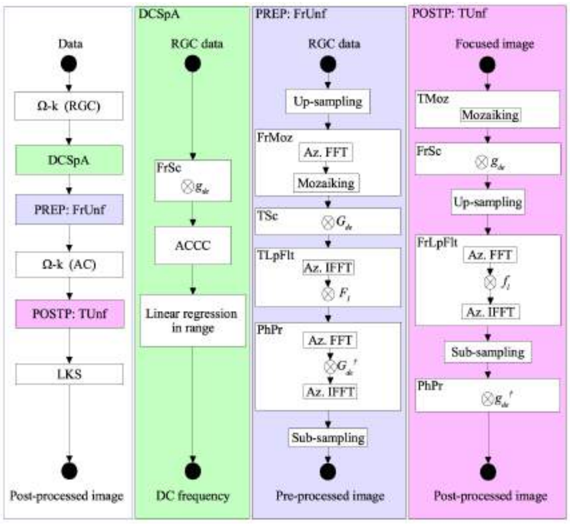

Figure 2: Block diagram of the proposed TOPS processor. See text for acronyms.

It is known that the Ω-k algorithm involves range compression (RGC), then azimuth compression (AC) followed by look summation (LKS) either for multi-looking or to remove the azimuth focusing shift. For TOPS, this is preceded by the FrUnf pre-processing (PREP) and followed by the TUnf post-processing (POSTP). The literature describes these steps assuming that the DC frequency (i.e., the squint angle) at the middle of the burst ($f_{tc,0}$) is zero. In general, this is not the case, and all processing components described below shall be based on this more realistic assumption. Moreover, a stage is added before PREP for estimating the initial DC frequency by spectral analysis (DCSpA). This stage is applied after RGC. Since RGC and PREP process along orthogonal directions (range and azimuth, respectively), they commute. Therefore, to efficiently implement DC estimation, our TOPS processor is decomposed into the following successive stages: RGC, DCSpA, PREP, AC, POSTP, and LKS. Accordingly, spectral analysis for DC estimation is carried out on the range-compressed data for better accuracy.

The frequency scaling (FrSc) performs de-rotation of the azimuth TFDi and cancels the azimuth dependence of the DC frequency that becomes the constant $f_{tc,0}$. Figure 3 shows the effect of FrSc in the time-frequency domain (TFD). The left part represents the support of the RGC data without AzFrF. FrSc consists in multiplying each column of the data by the de-rotation function. If $f_{tc,r}$ denotes the range-dependent slope of the DC along the azimuth direction (the DC rate), this function is given by

$$g_{de}(t,r) = \exp\left(-j\pi f_{t_{c,r}}(r) t^2\right). \quad (1)$$

The spectral analysis is based on the Average Cross Correlation Coefficient (ACCC) algorithm [15]. Linear regression in range provides $f_{tc,0}$ as a linear function of range.

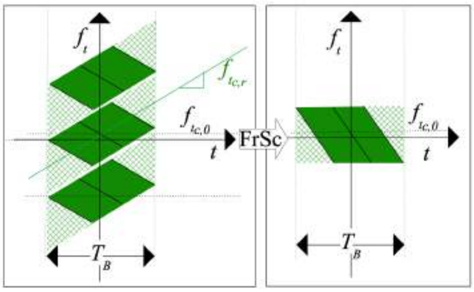

Figure 3: FrSc in the TFD.

Frequency un-folding (FrUnf) resolves the AzFrF by replicating the data along the azimuth frequency axis so that there is no frequency aliasing anymore. The up-sampling (UpSamp) stage allows to increase the initial number of azimuth pixels to the nearest larger integer power of two in view of the azimuth FFT. The purpose of frequency mozaiking (FrMoz) is to replicate the TFDi so that the frequency extent becomes a multiple of v_t. The time scaling (TSc) permits to reduce the azimuth time extent of each replicate. To cancel the aliased contributions in the TFDi, low-pass filtering in the time domain (TLpFlt) is performed. The step of phase preservation (PhPr) permits to recover the initial phase. Then sub-sampling (SubSamp) permits to reduce the slow-time extent to the initial one, i.e., T_B. Figure 4 shows the effect of PREP in the TFD for N_{ff}=3.

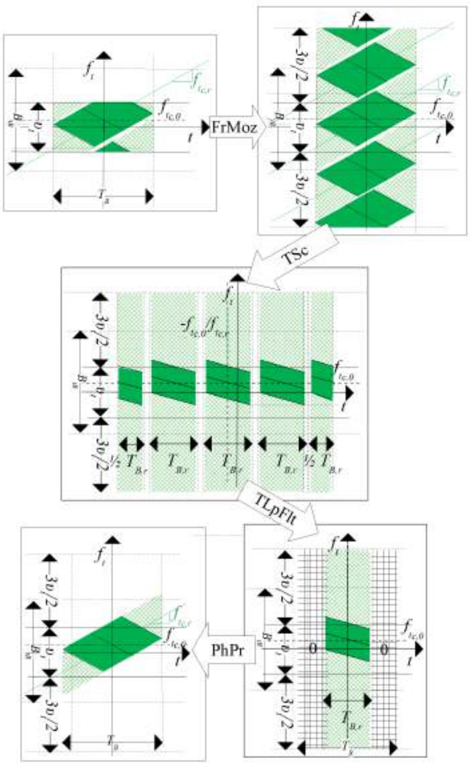

Figure 4: PREP (FrUnf) in the TFD.

TSc consists in multiplying in the frequency domain (FD) each column of the data by the function G_{de} defined as

$$G_{de}(f_t, r) = \exp\left(j\pi(f_t - f_{tc,0})^2 / f_{tc,r}\right). \quad (2)$$

TSc reduces time extent. It thus provides what we call reduced burst time : $T_{B,r} = v_t/2f_{tc,r}$. To cancel the aliased contributions in the TFDi, TLpFlt uses a low-pass filter F_l only keeping times in the range [$-T_{B,r}/2$, $T_{B,r}/2$].

If α denotes the mode factor, focusing results in dividing the slope of the line of DC frequencies by α:

$$f'_{tc,r} = f_{tc,r}/\alpha. \quad (3)$$

This increases the slow time extent by the same factor: $T_{of} = (T_B - T_D)\ \alpha$ and results in the time folding problem. Moreover, the time center is shifted at position

$$t_{c,0} = f'_{tc,r}/f'_{tc,0}. \quad (4)$$

TUnfr solves AzTF by replicating the data along the azimuth time axis so that there is no aliasing in time anymore. It can be seen that both TUnf and FrUnf unfolding processings work in the same way, they only differ by the axis on which the folding is resolved (the time axis for PREP, and the frequency axis for POSTP).

The purpose of time mozaiking (TMoz) is to replicate the TFDi so that the time extent becomes a multiple of the initial one. The purpose of frequency scaling (FrSc) is to reduce the azimuth bandwidth of each replicate. Then, UpSamp has the same goal as for PREP. To cancel the aliased contributions in the TFDi, low-pass filtering in the frequency domain (FrLpFlt) is performed. SubSamp permits to reduce the slow-time extent to the initial one during POSTP. Then, PhPr has the same goal as for PREP. Figure 5 shows the effect of POSTP in the TFD for N_{ft}=2.

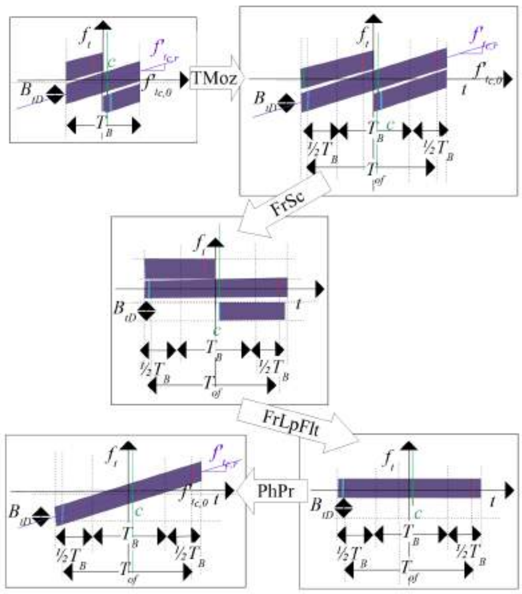

Figure 5: POSTP (TUnf) in the TFD.

FrSc reduces the azimuth bandwidth of each replicate by multiplying in the time domain (TD) each column of the data by the de-rotation function g_{de} given by

$$g_{de}(t,r) = \exp(-j\pi f'_{t_{c,r}}(t + t_{c,0})^2). \qquad (5)$$

To cancel the aliased contributions in the TFDi, FrLpFlt uses a low-pass filter f_l cancelling the frequencies outside the frequency range [- B_{tD} /2, B_{tD}/2].

3 Results

We focused a full Sentinel-1 scene acquired over a site centered on Verdun in France and covering a south part of Belgium on January 12, 2015. This acquisition contains 3 sub-swaths. The effective azimuth bandwidth ($B_{tB,e}$) is almost 4 times larger than v_t and the output time extent is more than 4 times larger than the burst time (see Table 2).

Parameter	IW1	IW2	IW3
Number of valid bursts	11	11	11
Azimuth beam-width (rad)	0.0051	0.0035	.0047
Effective velocity (m/s)	7174.4	7378.05	7614.6
Slow-time sampling frequency	1717.1	1451.6	1685.8
Antenna sweep rate (rad/s)	-0.029	-0.018	-0.027
Burst time (s)	0.82	1.07	0.84
Effective azimuth bandwidth	5947.5	5024.1	5960.6
Output time extent (s)	3.33	3.15	3.35

Table 2: Main swath-dependent SAR parameters, computed at mid-range for each sub-swath.

Figure 6 shows the results of the proposed processor on Sentinel-1 data (first sub-swath, first burst). There is no azimuth aliasing anymore.

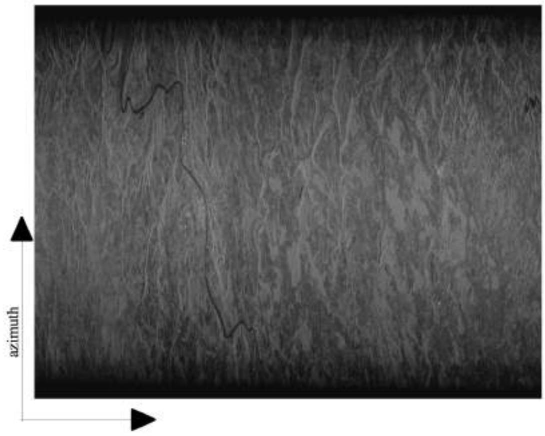

Figure 6: Results of the proposed processor on Sentinel-1 data (first sub-swath, first burst).

Figure 7 shows the azimuth spectrum of the same burst after different stages of the reconstruction (RGC, PREP, AC, and POSTP.) The lines in turquoise show the DC frequencies (as estimated by DCSpA for RGC and PREP, and computed with formula (3) for AC and POSTP). The resolving of AzFrF by PREP and of AzTF by POSTP is clearly visible.

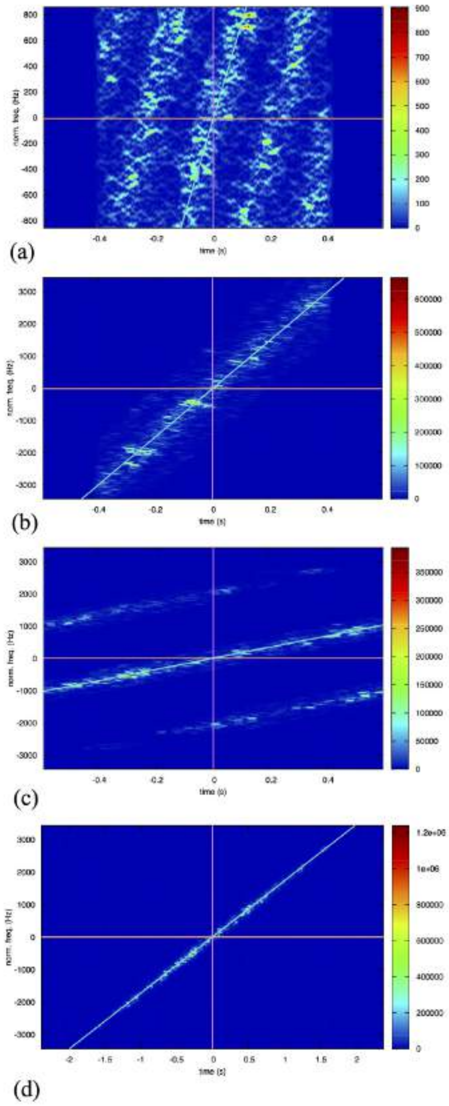

Figure 7: Azimuth spectrogram of the results on the same burst after (a) RGC, (b) PREP, (c) AC, (d) POSTP.

4 Conclusions

A TOPS processor has been presented and tested using Sentinel-1 data. It is based on a full-aperture method that combines a pre-processing that solves the azimuth frequency folding, Omega-K focusing, and a post-processing that solves the azimuth time folding. Further work is in progress to consolidate the processor and to interface it with a Sentinel-1 Wide-Swath InSAR processor that we are developing in the framework of a parallel research contract.

Acknowledgments

This work has been funded by Belspo. We also thank N. Miranda of ESA-ESRIN for the helpful discussions.

References

[1] R. K. Moore, J. P. Claassen and Y. H. Lin, "Scanning Spaceborne Synthetic Aperture Radar with Integrated Radiometer," *Aerosp. Electron. Syst. IEEE Trans. On*, vol. AES-17, no. 3, pp. 410–421, May 1981.

[2] A. Monti Guarnieri and C. Prati, "ScanSAR focusing and interferometry," *Geosci. Remote Sens. IEEE Trans. On*, vol. 34, pp. 1029–1038, 1996.

[3] J. Holzner and R. Bamler, "Burst-mode and ScanSAR interferometry," *Geosci. Remote Sens. IEEE Trans. On*, vol. 40, pp. 1917–1934, 2002.

[4] A. Moreira, J. Mittermayer and R. Scheiber, "Extended chirp scaling algorithm for air- and spaceborne SAR data processing in stripmap and ScanSAR imaging modes," *Geosci. Remote Sens. IEEE Trans. On*, vol. 34, pp. 1123–1136, 1996.

[5] F. D. Zan and A. M. Guarnieri, "TOPSAR: Terrain Observation by Progressive Scans," *Geosci. Remote Sens. IEEE Trans. On*, vol. 44, pp. 2352–2360, 2006.

[6] E. Attema, M. Davidson, N. Floury, G. Levrini, B. Rosich, B. Rommen and P. Snoeij, "Sentinel-1 ESA New European Radar Observatory," in *Synthetic Aperture Radar (EUSAR), 2008 7th European Conference on*, 2008, pp. 1–4.

[7] P. Prats, R. Scheiber, J. Mittermayer, A. Meta, A. Moreira and J. Sanz-Marcos, "A SAR processing algorithm for TOPS imaging mode based on extended chirp scaling," presented at the Geoscience and Remote Sensing Symposium, 2007. IGARSS 2007. IEEE International, 2007, pp. 148–151.

[8] P. Prats, R. Scheiber, J. Mittermayer, A. Meta and A. Moreira, "Processing of Sliding Spotlight and TOPS SAR Data Using Baseband Azimuth Scaling," *Geosci. Remote Sens. IEEE Trans. On*, vol. 48, pp. 770–780, 2010.

[9] P. Huang and W. Xu, "An efficient imaging approach for tops SAR data focusing based on scaled Fourier transform," *Prog. Electromagn. Res. B*, vol. 47, pp. 297–313, 2013.

[10] J. Mittermayer, A. Moreira and O. Loffeld, "Spotlight SAR data processing using the frequency scaling algorithm," *Geosci. Remote Sens. IEEE Trans. On*, vol. 37, pp. 2198–2214, 1999.

[11] X. Bai, J. Sun, W. Hong and S. Mao, "On the TOPS mode spaceborne SAR," *Sci. CHINA Inf. Sci.*, pp. 367–378, 2010.

[12] D. Guo, Xu H and Li J, "Extended wavenumber domain algorithm for highly squinted sliding spotlight SAR data processing," *Prog. Electromagn. Res. B*, vol. 114, pp. 17–32, 2011.

[13] G. Sun, M. Xing, Y. Wang, Y. Wu, Y. Wu and Z. Bao, "Sliding Spotlight and TOPS SAR Data Processing Without Subaperture," *Geosci. Remote Sens. Lett. IEEE*, vol. 8, pp. 1036–1040, 2011.

[14] W. Xu, P. Huang and Y. Deng, "TOPSAR data focusing based on azimuth scaling preprocessing," *Adv. Space Res.*, vol. 48, pp. 270–277, 2011.

[15] I. Cumming and F. Wong, *Digital Processing of SAR Data*, Artech House, Norwood, MA. 2005.

[16] G.-C. Sun, M. Xing, X.-G. Xia, Y. Wu and Z. Bao, "Beam Steering SAR Data Processing by a Generalized PFA," *Geosci. Remote Sens. IEEE Trans. On*, vol. 51, pp. 4366–4377, 2013.

[17] G.-C. Sun, M. Xing, X.-G. Xia, J. Yang, Y. Wu and Z. Bao, "A Unified Focusing Algorithm for Several Modes of SAR Based on FrFT," *Geosci. Remote Sens. IEEE Trans. On*, vol. 51, pp. 3139–3155, 2013.

ISBN 978-3-8007-4228-8 / ISSN 2197-4403